Commission no. VII/9

V. C. Vanderbilt
B. F. Robinson
L. L. Biehl
M. E. Bauer
A. S. Vanderbilt

Purdue University
Laboratory for Applications of Remote Sensing
West Lafayette, Indiana USA

Simulated Response of a Multispectral Scanner Over Wheat as a Function of Wavelength and View/Illumination Directions

ABSTRACT

Oblique viewing sensors have been proposed for the Multispectral Resource Sampler (MRS), a follow-on satellite to the Thematic Mapper/Landsat D and proposed by the United States for launch in the late 1980's. If an oblique viewing sensor is to be included on the MRS, then the potential information in oblique measurements needs to be better understood.

This paper analyzes the reflectance response with view angle of wheat, excluding atmospheric effects but otherwise simulating the response of a multispectral scanner. The analysis is based upon spectra taken continuously in wavelength from 0.45 to 2.4 μm at more than 1200 view/illumination directions using an Exotech model 20C spectral radiometer. Data were acquired six meters above four wheat canopies, each at a different growth stage.

The analysis shows that the canopy reflective response is a pronounced function of illumination angle, scanner view angle, and wavelength. The variation is greater at low solar elevations compared to high solar elevations.

INTRODUCTION

Oblique viewing sensors have been proposed or scheduled for launch on at least two future earth resource satellite systems, the Système Probatoire d'Observation de la Terre[1] (SPOT) being developed in association between France, Sweden, and Belgium and the Multispectral Resource Sampler[2] (MRS) being developed by the United States. As these sensors are soon to be launched, the potential information in oblique measurements needs to be anticipated and better understood.

The spectral flux sensed by these systems will be due to the absorption and bidirectional scattering of solar radiation by both the atmosphere and ground scene. Characterization and correction of the effect of the atmosphere upon remotely sensed data have been considered elsewhere.[3] This paper analyzes the spectral bidirectional scattering properties of wheat with view direction, excluding atmospheric effects.

If the ground scene is a level and a perfectly diffuse reflector, a Lambertian surface, then the response of the sensor will not vary with view angle, provided atmospheric effects may be neglected. However, never is an extended natural surface level and Lambertian; inevitable surface roughness

is responsible for light and dark surface areas and the consequent variation in the sensor response with view angle. The roughness inherent in a plant canopy provides an example of this process; the presence of shadows, cast by foliage, in differing proportions depending upon view angle suggests that the canopy is not a Lambertian reflector, that the sensor response will not be constant with canopy view angle.

The reflective response of a vegetative canopy has been modeled[4,5,6] using physically based parameters such as leaf area index, leaf areas projected in particular directions, probability density functions of leaf area with angle, probability of gap, reflectance and transmittance of canopy components, index of refraction, etc. Analyses and parameter studies have investigated the predictions and properties of the models and, based on the models, offered insight into the canopy reflectance process.[4,5,7,8,9] Very limited field verification of the models has been reported.

Measurements of an information class such as wheat or corn made by multispectral scanners mounted in aircraft often show large variation with scan angle. For example, during the Corn Blight Watch Experiment, the size of the variation was sufficient to require preprocessing to remove the effect.[10] The response of the aircraft sensors, which typically operate over angular variations of $\pm 40^{o}$ about nadir, include variations due not only to bidirectional scattering by the ground scene but also due to the atmosphere. Consequently, data from the sensors cannot be interpreted as completely indicative of the ground scene.

Measurements of the bidirectional scattering properties at large view angles for various plant canopies have been reported.[9,11] None of these studies involved measurements made continuously in wavelength from 0.4 to 2.4 μm and at a variety of view angles and crop growth stages. Nor have these studies extensively investigated the reflective properties of wheat, a crop of global economic importance grown worldwide.

MATERIALS AND METHODS

Data were acquired on wheat (Triticum aestivum L.) on four dates during 1975 and 1976 at Williston, North Dakota, USA (Lat. $48^{o}8'$, Long. $103^{o}44'$) in support of the Large Area Crop Inventory Experiment (LACIE).[12] On each date agronomic measurements were made to characterize the condition of the wheat canopy (Table 1). Meteorologic data (Table 1) were acquired at the North Dakota Agricultural Experiment Station at Williston, located near the test sites.

All spectral data were acquired continuously in wavelength 0.46 to 2.4 μm, using an Exotech model 20C spectroradiometer[13] (Exotech, Inc., Gaithersburg, Maryland) positioned 6 m above the soil and bolted to a pan head mounted to a boom supported by a truck (Figure 1). On each of the four dates, the truck and associated instrument van and electrical generator were located amidst the wheat and sufficiently distant from field edges to uniformly fill for all view directions the 15^{o} field of view of the spectroradiometer. Spectral data and a photograph of the instrument field of view were taken in each of 33 view directions, eight azimuths (the eight points of the compass) at four zenith angles (15^{o}, 30^{o}, 45^{o} and 60^{o}) plus nadir. On each day data were acquired approximately from three hours before solar noon to four hours after solar noon. The spectral data, acquired as radiances, were subsequently calibrated to bidirectional

reflectance factors (BRF)[14] using spectral radiance measurements taken periodically of a 1.1 m x 1.1 m barium sulfate ($BaSO_4$) painted field standard.[15] The reflectance of the field standard was measured with reference to pressed $BaSO_4$, a laboratory standard with known reflective properties.[16]

Spectral data and corresponding wavelength information were simultaneously recorded on analog frequency modulated magnetic tape and on a multiple channel strip chart recorder. A crystal frequency controlled power source maintained tape transport speed specifications. On play back in the laboratory, the analog signals were sampled, digitized, and then converted to bidirectional reflectance factors using algorithms implemented on IBM 370/148 and IBM 3031 computers.

The field of view photographs, taken with each spectra, were used to assess spectral data quality. A spectra was discarded for analysis purposes if the associated photograph indicated the field of view of the instrument might include the shadow cast by the spectroradiomater, boom, or truck or in some way did not properly represent the scene.

Analysis of the bidirectional response of the canopy was performed on data at 48 wavelengths selected at 0.02 μm intervals from 0.44 to 1.0 μm, at 0.04 μm intervals from 1.0 to 2.0 μm, and at 0.08 μm intervals from 2.0 to 2.24 μm. The wavelengths were chosen to concentrate analysis efforts in the visible spectral region. At a particular wavelength the spectral resolution of the data is better than 2.6% of that wavelength.

At each of the 48 wavelengths, a stepwise forward regression program was used in a two part sequence to select from a global set of possible terms the twenty which best explained the variation in the BRF data with time and view angle (Figure 2). The global set included the terms of the spherical harmonic series[17] through Y_{40}, powers of time through t^6, and all the interaction terms. The number of terms in the global set was first reduced by analyzing regression results at 10 wavelengths strategically placed across the spectrum and selecting from the global set those terms explaining most of the variation in the data. Because analysis of residuals indicated additional terms were needed to correctly model large variations in the BRF in the visible spectral region at view angles near

Figure 1. The Purdue/LARS field spectroradiometer system.

nadir, three terms, each having a Gaussian response with view angle, were added to the select set of terms. Next a program for the regression of the data at each wavelength chose the best twenty terms from the select set and determined the coefficients of the regression equations.

Analysis of the residuals of the twenty term regressions revealed no significant pattern as a function of the following variables: time, view zenith, view azimuth, sun zenith, sun azimuth, predicted BRF, and measured BRF. The coefficient of variation (R^2) of each regression varied systematically by date and wavelength, ranging between 0.86 and 0.98 in the visible spectral region, 0.93 and 0.98 in the near-infrared and 0.76 and 0.96 in the middle-infrared. The standard deviation of the quantity (100% residual/measured) varied between 3.5% and 10.7% in the visible spectral region, 2.5% and 5.2% in the near-infrared, and 3.3% and 16.4% in the middle-infrared.

The coefficients of the regression equations at the 48 wavelengths and four dates were processed by computer into a computer program for exercizing the equations to perform parameter studies. Additional computer programs were written to plot the calculated values on a computer line printer. The resultant curves were traced and labeled by hand, photographically reduced, and assembled into arrays of plots.

RESULTS

The normalized BRF of wheat was plotted as a function of wavelength and view direction, at three times during the day, and for four crop development stages. The analysis assumes there are no atmospheric effects.

Figure 3 shows the normalized BRF plotted as a function of wavelength for the wheat canopy measured 21 June 1976 three hours before noon looking 90^{o} to the sun azimuth. The BRF is normalized to the BRF at nadir at each wavelength. The scale on the wavelength axis changes at 1.0 and 2.0 μm. Figure 3 shows that the BRF is a pronounced function of view zenith direction and wavelength. In the green spectral region (0.56 μm) the BRF decreases for view zenith directions between 0 and about 20^{o} then increases for angles greater than 30^{o}. In the red region (0.66 μm) the BRF decreases until a view zenith direction of 40^{o}, then is constant. In the near-infrared (0.76-1.28 μm) the BRF increases with increasing view zenith angle. In the middle-infrared at 1.68 μm the BRF response is like that in the green region while at 2.16 μm the response is similar to that in the red spectral region.

The results shown in Figure 4 represent the normalized BRF of the canopy on one date 17 July 1976 three hours before noon. The results in Figure 4 are based on the simulated response of a conical scan, normalized to 1.0 at the canopy hot spot, the antisolar point, and scanning in azimuth angle with the zenith view angle fixed at the angle of the canopy hot spot. The results were obtained by dividing the wavelength axis into three wavelength regions, visible 0.44-0.68 μm, near-infrared 0.76-1.28 μm, and middle-infrared 1.48-1.76 μm and 2.08-2.24 μm. On Figure 4 the range of the canopy BRF responses in each wavelength region is signified by the appropriate stippled area. For example, at an azimuth angle of -90^{o}, the BRF in the visible region ranged between 0.5 and 0.55 of the BRF at the hot spot. Figure 4 shows that the response as a function of azimuth angle measured from the hot spot is symmetric and decreases. The decrease of the response is greatest in the visible region and least in the near-

infrared region.

Figure 5 shows the wavelength and scan angle scales which apply to each plot in the 3 x 4 array of plots in Figures 6a and 6b. The wavelength scale changes at 1.0 and 20 μm. The scan angle scale is organized for data from a multispectral line scanner scanning ±60° about nadir. Negative scan angles are zenith angles to the left of nadir.

Figure 6 shows the BRF response of a MSS normalized to the response at nadir and scanning ±60° about nadir. The wavelength and zenith scan angle scales of each of the 24 plots in Figure 6 are illustrated in Figure 5. Each line of plots in Figure 6 represents a particular time. Each column of plots in Figure 6 represents a specific crop development stage. In each plot the normalized BRF at a particular scan angle and wavelength is indicated by the height quantized in topographic notation by contour lines at 0.1 unit intervals. The BRF on a contour line labeled 1.1 is 1.1 times the BRF at nadir. The contour line immediately adjacent to the line labeled 1.1 indicates a BRF value of either 1.0, 1.1, or 1.2 times the nadir BRF, depending on the sequence of contour lines.

The results in Figure 6a, the case of the MSS-equipped aircraft flying toward the solar azimuth, show the normalized BRF with scan angle is generally symmetrical about the nadir scan angle for all wavelengths, all three times, and all four growth stages. For example, the BRF for [scan angle = ±60°, ±3 hours, 21 June 1976, λ=0.64 μm] is 0.6 of the BRF at nadir at 0.64 μm; similarly, the BRF at 0.8 μm is 1.4 of the BRF at nadir for -3 hours and 1.5 of the BRF at nadir for +3 hours. In the near-infrared spectral region, the BRF generally increases with increasing scan angle for all three times and all four crop development stages. In the visible and middle-infrared regions, a simple pattern doesn't exist; the BRF may increase or decrease depending upon wavelength, illumination angle, and development stage.

Figure 6a also shows the BRF with scan angle for three hours before noon is very similar to the response three hours after noon, suggesting that the BRF is fairly symmetric not only in scan angle but also with illumination angles from noon. Generally, for a particular wavelength, whatever changes that do occur with scan angle are enhanced at the two times away from noon as compared to noon. In each plot the transition between the visible and near-infrared spectral regions is abrupt for the green, healthy canopies (columns labeled 21 June 1976, 20 July 1975, and 17 July 1976) and markedly less so for the senescent canopy (column labeled 31 July 1976) without the strong red chlorophyll absorption band.

Figure 6b, the case of the aircraft flying in a direction 90° to the sun azimuth direction, reveals a BRF similar to that of Figure 6a. The same transition phenomenon is evident at 0.7 μm between the visible and the near infrared regions. The curves are fairly symmetric with illumination angle from noon. In the near-infrared region, the BRF generally increases for increasing scan angles regardless of crop development stage or time. (Note the minor but systematic exception to this rule near nadir where the BRF is between 0.9 and 1.0 of nadir BRF.) However, unlike Figure 6a the response curves of Figure 6b are not symmetric with scan angle.

DISCUSSION

The results, Figure 4, are consistent with the concept that the effects of shadowing on BRF are modulated by the effects of light multiply scattered by canopy components. Radiation is multiply scattered when it is reflected or transmitted more than one time by foliage or soil in the canopy. Light tends to be multiply scattered in crop canopies in regions of the spectrum where the foliage absorbs little light (i.e., the near infrared band from 0.8 μm to 1.3 μm) and tends to not be multiply scattered in regions of the spectrum where foliage absorbs a significant proportion of the incident light (i.e., the red wavelength band prior to senescence). Multiply scattered light tends to reduce the contrast between two adjacent surfaces in the canopy, one surface illuminated by direct solar radiation and the other surface shadowed. The BRF of a crop canopy is the sum of the individual contributions of the shadowed and illuminated surface areas in the canopy. If the contrast between the shadowed and illuminated areas is negligible, then changes in the proportion of shadowed surface area to illuminated surface area in the canopy will not be evident in the canopy BRF. Conversely, if the contrast is significant, then changes in the proportion of shadowed to illuminated surface area in a canopy will be evident as changes in the canopy BRF. Therefore, the canopy BRF is a function of both the proportion of shadowed to illuminated surface area in the canopy and the importance to the canopy radiation environment of multiply scattered light, which reduces the contrast between the shadowed and illuminated surface areas.

The results, Figure 4, are for one zenith view angle, that of the hot spot. If the canopy foliage were randomly distributed both spatially and azimuthally, then, because the zenith view angle is constant, the relative proportions of the canopy components in the field of view of a sensor would not change with azimuth scan angle. The proportion of illuminated to shadowed foliage would be greatest at the hot spot, an azimuth scan angle of zero, and least at an azimuth scan angle of 180^{o}. If the BRF of the canopy were merely a function of the proportion of illuminated to shadowed foliage, then the stippled areas of Figure 4 should coincide. That the regions do not coincide indicates other factors must be included in the analysis.

At any azimuth scan angle away from the hot spot, the stippled areas are ordered from top to bottom, near-infrared, middle-infrared, and visible. The ranking corresponds with a ranking of the importance of multiply scattered light in each spectral region. Each stippled area representing a spectral region is almost symmetric with azimuth scan angle from the hot spot; the proportion of illuminated to shadowed areas is similarly symmetric provided the canopy foliage is randomly distributed. Consequently, the results, Figure 4, are consistent with the argument that the effects of multiply scattered light serve to modulate the effects of shadowing on the BRF of the canopy.

The results, Figure 3 and 6, are consistent with the argument that shadows cast by foliage are an important factor in the variation of BRF with view direction. Considering Figure 6a, the proportion of shadowed to sunlit foliage and soil should be approximately the same at equal angles left and right of nadir provided the foliage is randomly distributed. Since the BRF of a crop canopy is the sum of the individual contributions of the shadowed and illuminated surface areas in the canopy, then the BRF should be symmetrical in scan angle from nadir--as it is in Figure 6a, regardless of wavelength. Considering Figure 6b, the curves are asymmetric

in scan angle about nadir. At all wavelengths, the normalized sensor response is noticeably larger on the side of the flightline away from the sun, toward the canopy hot spot where shadows cast by foliage would not be seen. Shadows cast by foliage would be observable on the opposite side of the flightline, the side with the lower response indicated by Figure 6b. Thus, the results support the argument that shadowing is an important factor in the variation of BRF with view direction.

The results, Figure 6, are consistent with the argument that shadows cast by foliage are an important factor in the variation of BRF not only with view direction but also with illumination angle. The proportion of shadowed to illuminated surface areas in a canopy changes with sun angle during the day. The proportion varies from unity (all shadow) at sunrise and sunset to a low value sometime during the day. For a particular view fixed relative to the illumination direction, the proportionality, a function in time, will be symmetric about solar noon if the azimuthal orientation and spatial distribution of the foliage is symmetric about a north-south line and if confounding factors (i.e., phototropism, plant geometry changes due to wind or moisture stress, etc.) are not important. For a particular view direction fixed relative to the sun direction, the BRF should, in general, be symmetric in time and sun angles about solar noon. provided (1) the geometry of the canopy remains properly symmetric throughout the day and (2) the spectral properties of the canopy components are constant or vary symmetrically in time about solar noon. (For example, if significant soil surface dry down occurred during a day, then the canopy would fail to satisfy criteria 2 when the soil reflectance changes, in any, were asymmetric about solar noon.) The results, Figures 3 and 6, show the BRF for a particular wavelength and scan angle is generally symmetric in time about solar noon, supporting the argument that shadowing is an important factor for explaining the variation in BRF with illumination angles.

The results, Figures 3 and 6, are consistent with the idea that the BRF changes in certain ways with scan angle because the probability of observing the various components of the canopy changes significantly with scan angle. For example, the probability of observing bare soil is generally greatest at nadir and decreases rapidly with increasing scan angle across the canopy. Figure 3 and several plots in Figure 6 reveal an abrupt change of BRF with scan angle near nadir for the visible spectral region, suggesting the effect of the soil should be considered for understanding the properties of the BRF under these conditions. As a second example, for most canopies at large scan angles only the upper layers of the canopy are visible. The upper layers of a canopy are well illuminated --no higher foliage shadows the topmost layer. Thus, at large, incrementally increasing scan angles the proportion of shadows should decrease and the BRF should increase. Figures 3 and 6 reveal such a pattern in the near-infrared spectral region of all plots and in the visible portions of several plots. The pattern may exist throughout the visible spectral region where the BRF might increase at scan angles larger than the 60° measured.

ACKNOWLEDGEMENT

This research could not have been performed without the generous, timely, and friendly assistance of E. French, manager, and the staff of the North Dakota Agricultural Experiment Station at Williston, North Dakota. Additional thanks are expressed to A. Owan, P. Farris, and L. O'Neill, owners of the wheat fields used in the experiment. Acquisition and processing of spectral data were supported by the National Aeronautics

and Space Administration under contracts NAS9-14016 and NAS9-14970. Portions of the data analysis were supported by the National Aeronautics and Space Administration under contract NAS9-15466.

REFERENCES

1. M. Chevrel, M. Courtois, and G. Weill, "The SPOT satellite remote sensing mission," Proc. 1980 ACSM-ASP Convention, St. Louis, Missouri.

2. C. C. Schnetzler and L. L. Thompson, "Multispectral Resource Sampler: an experimental satellite sensor for the mid-1980's," Proc. SPIE Technical Symp., vol. 183, Huntsville, Alabama, May 1979.

3. R. E. Turner and M. M. Spencer, "Atmospheric model for correction of spacecraft data," Proc. of 8th Int. Symp. Remote Sensing of Environment, Ann Arbor, Michigan, pp. 895-934, Oct. 1972.

4. G. H. Suits, "The calculation of the directional reflectance of a vegetative canopy," Remote Sensing of Environment, vol. 2, pp. 117-125, 1972.

5. J. A. Smith and R. E. Oliver, "Plant canopy models for simulating composite scene spectroradiance in the 0.4 to 1.05 micrometer region," Proc. 8th Int. Symp. on Remote Sensing of Environment, Ann Arbor, Michigan, pp. 1333-1354, 1972.

6. V. C. Vanderbilt, "A model of plant canopy polarization response," Symp. on Machine Processing of Remotely Sensed Data, W. Lafayette, Indiana, June 1980.

7. J. E. Colwell, "Vegetation canopy reflectance," Remote Sensing of Envir., vol. 3, pp. 175-183, 1974.

8. N. J. J. Bunnik, The multispectral reflectance of shortwave radiation by agricultural crops in relation with their morphological and optical properties, Wageningen: H. Veenman & Zonen B.V., 1978.

9. J. E. Chance and E. W. LeMaster, "Suits reflectance models for wheat and cotton: theoretical and experimental tests," Applied Optics, vol. 16, pp. 407-412, 1977.

10. R. B. MacDonald, M. E. Bauer, R. D. Allen, J. W. Clifton, J. D. Erikson, and D. A. Landgrebe, "Results of the 1971 Corn Blight Watch Experiment," in Proc. 8th Int. Symp. on Remote Sensing of Environment, Ann Arbor, Michigan, pp. 157-190, 1972.

11. K. T. Kriebel, "Das spektrale reflexionsvermögen einer bewachsenen oberfläche teil 1: methode und anwendung," Beiträge zur Physik der Atmosphäre, vol. 47, pp. 14-44, 1974.

12. M. E. Bauer, M. C. McEwen, W. A. Malila, and J. C. Harlan, "Design, implementation, and results of LACIE field research," in A Technical Description of the Large Area Crop Inventory Experiment (LACIE), The LACIE Symp., National Aeronautics and Space Administration, Johnson Space Center, JSC-16015, pp. 1037-1066, Oct. 1978.

13. R. W. Leamer, V. I. Myers, and L. F. Silva, "A spectroradiometer for field use," Rev. Sci. Instrum., vol. 44, pp. 611-614, 1973.

14. F. E. Nicodemus, J. C. Richmon, J. J. Hsia, I. W. Ginsberg, and T. Limperis, "Geometrical considerations and nomenclature for reflectance," National Bureau of Standards, U.S. Department of Commerce, NBS MN-160, 1977.

15. B. F. Robinson and L. L. Biehl, "Calibration procedures for measurement of reflectance factor in remote sensing field research," Measurements of Optical Radiation, SPIE, vol. 196, pp. 16-26, 1979.

16. F. Gram and G. W. Luckey, "Optical sphere paint and a working standard of reflectance," Applied Optics, vol. 7, pp. 2289-2294, 1978.

17. P. M. Morse and H. Feshbach, Methods of Theoretical Physics, New York: McGraw-Hill Book Co., 1953.

18. E. C. Large, "Growth stages in cereals," Plant Pathology, vol. 3, pp. 128-129, 1954.

Table 1. Ancillary meteorologic and agronomic data.

	Date			
Variable	21 Jun 76	20 Jul 75	17 Jul 76	31 Jul 76
relative humidity (%)	51	54	36	57
air temperature (C^o)	19	27	28	23
barometric pressure (mm Hg)	770.9	759.4	771.4	777.2
cloud cover (%)	1		1	5
wind direction	northeast	southwest	southeast	southeast
wind speed (km/hr)	14	16	10	13
cultivar	Waldron	Wells	Ellar	Ellar
maturity stage*	3.5/boot	4.5/fully headed	5.1/milk	5.4/ripe
row direction	east-west	east-west	north-south	north-south
row width (m)	0.18	0.21	0.18	0.18
fruit count (per m^2)	0.0		444.4	394.4
plant count (per m^2)	477.8	310.0	455.6	405.6
plant heigh (m)	0.48	0.72	0.85	0.86
leaves per plant	5.0		4.0	4.0
leaf condition (%)				
green	93		27	0
yellow	3		7	0
brown	4		66	100
dry biomass-total (gr/m^2)	216.9	345.1	689.8	625.9
fruit	0.0		268.1	330.2
green leaves	84.7		51	0.0
yellow leaves				
brown leaves			25.4	56.8
stems	132.3		345.3	238.9
fresh biomass-total (gr/m^2)	1131.1		1466.1	840.0
plant moisture (%)	81		53	25
leaf area index**	1.85	1.48	0.81	0.0

*maturity stage according to Large[18]
**leaf area index is the green one-sided leaf area per unit ground area

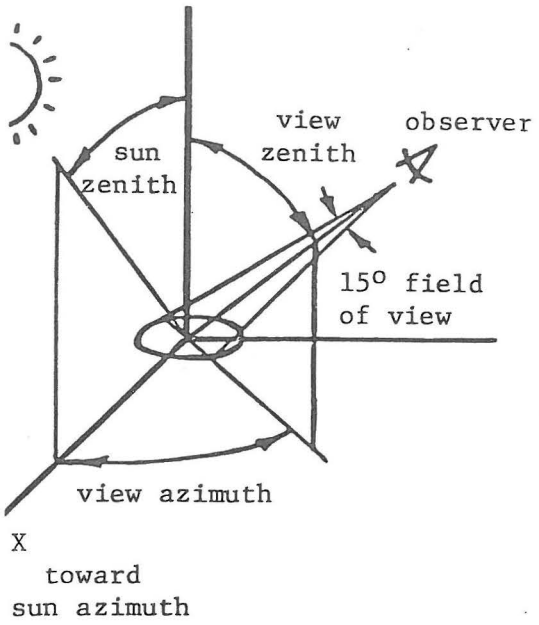

Figure 2. Coordinate system used for analysis.

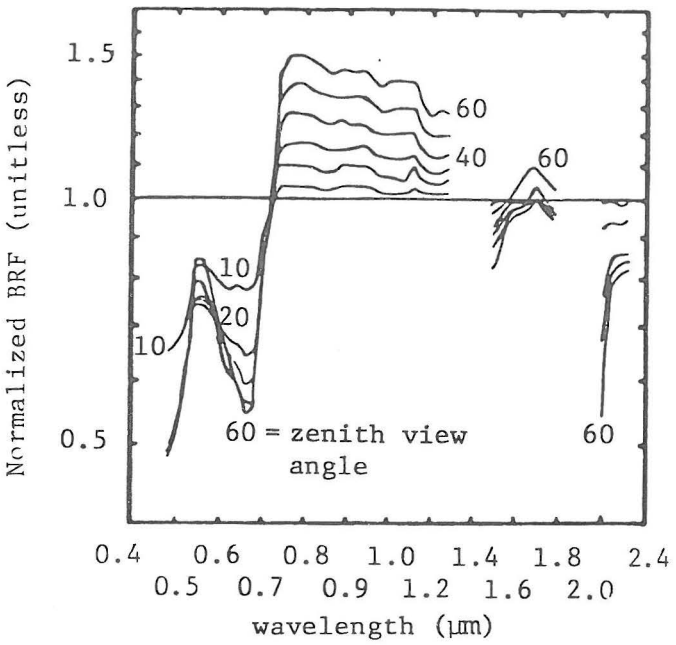

Figure 3. Normalized BRF for wheat 21 June 1976 three hours before noon with view azimuth 90° to sun azimuth. Sun (zenith, azimuth) = (43°,109°).

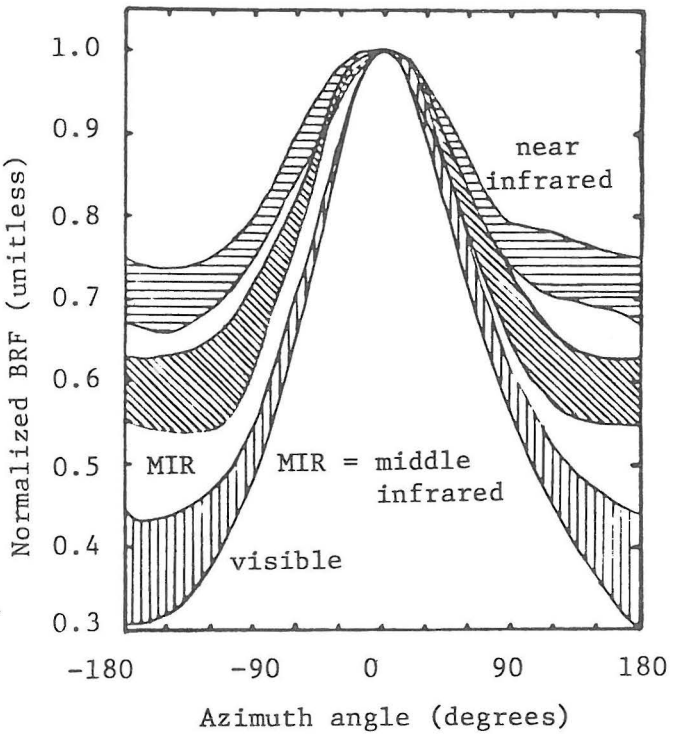

Figure 4. Normalized BRF for wheat 17 July 1976 three hours before noon. View azimuth angle is measured from hot spot.

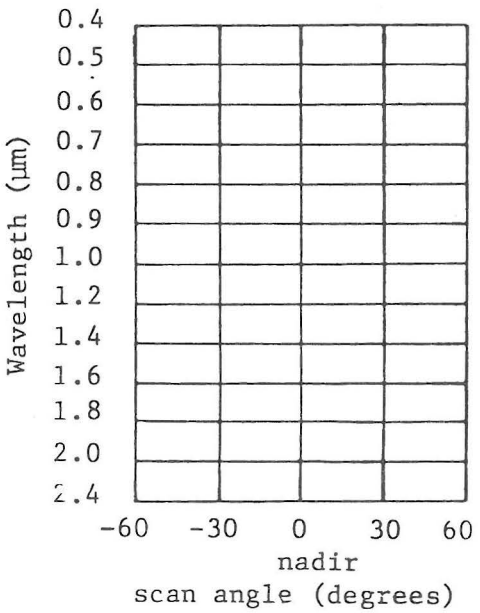

Figure 5. Coordinate system of each of the 24 plots in Figure 6. Wavelength scale changes at 1.0 and 2.0 μm.

Fig. 6a.

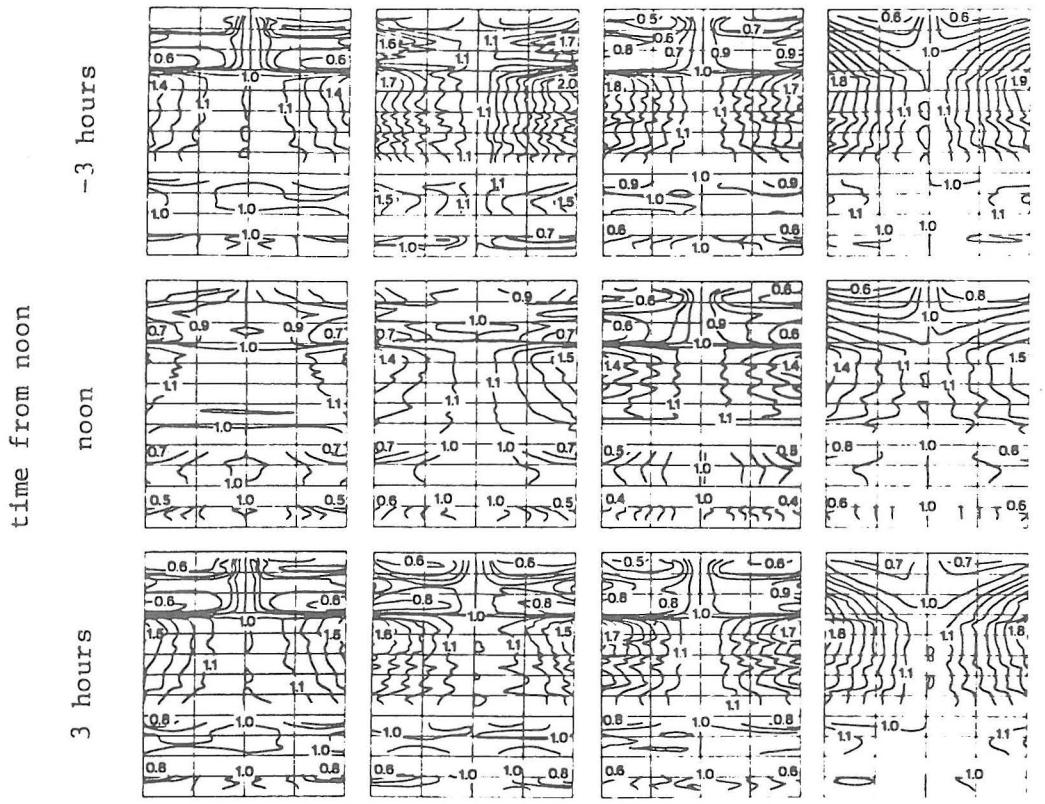

Fig. 6b.

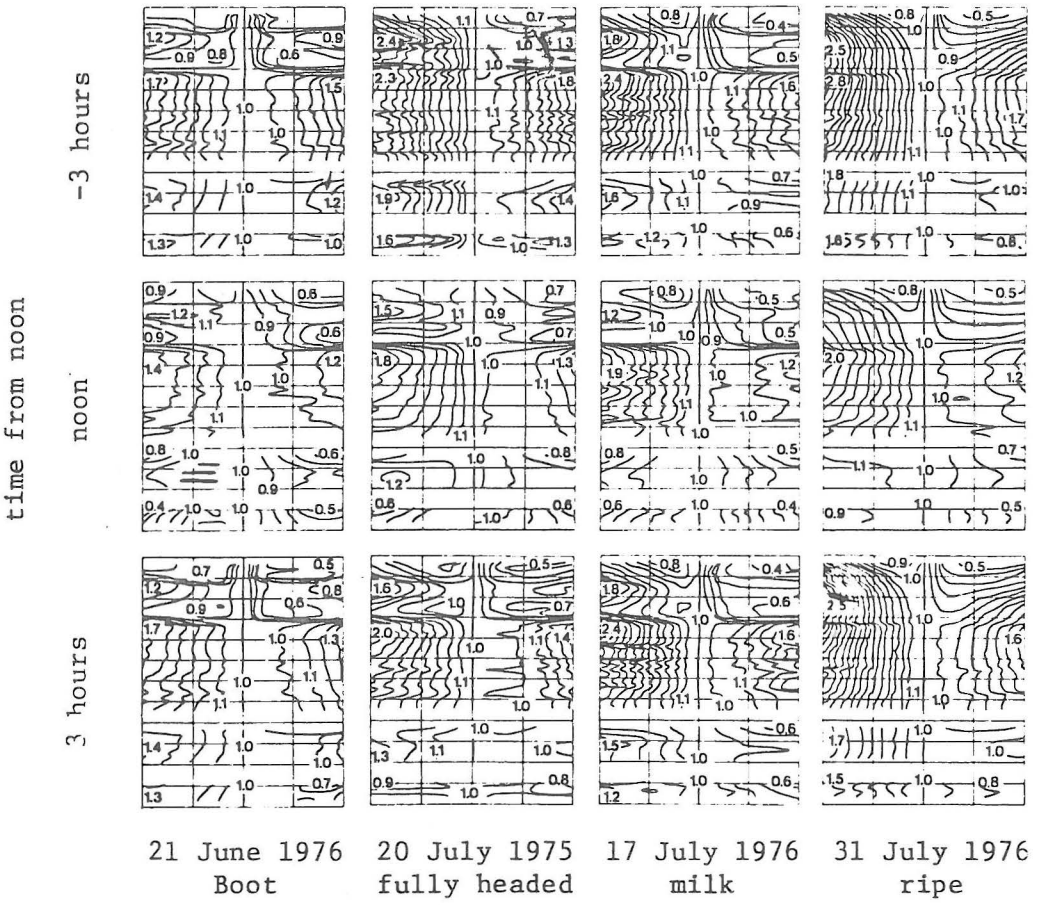

21 June 1976 Boot | 20 July 1975 fully headed | 17 July 1976 milk | 31 July 1976 ripe

Figure 6. Normalized BRF for a multispectral line scanner plotted in topographic notation with contour lines at 0.1 intervals.